Sys Rev Pharm 2020; 11(2): 372 – 381
A multifaceted review journal in the field of pharmacy
E-ISSN 0976-2779 P-ISSN 0975-8453

Etoposide-Loaded Gold Nanoparticles: Preparation, Characterization, Optimization and Cytotoxicity Assay

Maha M. Ali[1*], Nawal A. Rajab[1], Alaa A. Abdulrasool[1]
Department of Pharmaceutics, Collage of Pharmacy, University of Baghdad/Iraq
*E-mail: malakwissamsalim@gmail.com

Article History: *Submitted: 12.12.2019* *Revised: 09.01.2020* *Accepted: 10.02.2020*

ABSTRACT
In recent decades, gold nanoparticles are used for treatment and diagnosis of cancer through a myriad of modalities and delivery approaches. The aim of this study was to prepare and optimize etoposide-loaded gold nanoparticles by incorporated of etoposide in to the functionalized gold nanoparticles. Biocompatible polymers were used to enhance the colloidal stability, payloads capacity and cellular uptake. Twelve formulas were prepared and optimized by studying different variables such as nanoparticles size, etoposide loadig, polymer type, preparation temperature and sonicating duration on controlling size and uniformity of nanoparticles as well as etoposide loading efficiency and in-vitro release profile. The obtained results indicated that formula (F11) prepared from the functionalized gold nanoparticles (GN10) with a combination of HPMC-E5 and PVA (1:1), at room temperature and sonicating for 5 hours was selected as an optimized formula. F25 showed maximum etoposide loading capacity (1mg/ml) with higher loading efficiency (99.57%) and in-vitro released with controlled manner (better retardation at physiological pH ~ 7.4 and greater release at lysosomal pH ~ 4.6) as well as AFM results provided gold nanoparticles with smoother surface, average particles size (27.18nm) with uniform size distribution (15.02%). In addition to that, the result of TEM indicated uniform spherical shape with zeta potential of -39.23. In-vitro cytotoxicity studies showed high selectivity toward cancer (NHI-H69) than normal (BEAS-B2) cell lines. All these results gave a preliminary indication that etoposide-loaded gold nanoparticles considered as effective multiplexed therapeutic agent.

Keywords: Etoposide; Gold Nanoparticles; Polymer; Etoposide-Loaded Gold Nanoparticles; Particles Size; Distribution

Correspondence:
Maha M. Ali
Department of Pharmaceutics, College of Pharmacy
University of Baghdad, Iraq
E-mail: malakwissamsalim@gmail.com

DOI: 10.5530/srp.2020.2.55

INTRODUCTION
The discoveries in bio-nanotechnology over the course of past few years triggered a revolution in the field of medicine, delivering a profusion of novel approaches and actual applications of nano formulations for diagnosis and treatment of intractable diseases [1]. Accumulated evidence shows that smart metal nanoparticles such as gold, silver and copper can be used as a promising candidate particularly in the case of cancer and gene diseases [2]. From this perspective, Gold nanoparticles (GN) afforded an appealing platform for development of efficient multifunctional therapeutic, diagnostic, targeted delivery and controlled release systems [3].

The significant attention for GN grows because of their facile synthesis, chemical stability, functional flexibility, limited toxicity and biocompatibility. The possibilities to tuning the size, geometry and composition of gold nanoparticles by modifying the method of synthesis enables complete control of their unique optical and physicochemical properties [4].

Cancer is considered as a horrible disease and becoming a major cause of death despite significant investment and research [5]. Although large varieties of chemotherapies have been developed, unfortunately they have a lot of side effects. The construction of gold nanoparticles are recognized as an excellent intracellular targeting vector, tracked throughout the body by their visible light extinction behavior and can efficiently transport of drug molecules to the target sites with reduced dosage frequency and in (spatial/temporal) controlled manner to mitigate the side effects experienced with traditional therapies [6].

Etoposide is a potent chemotherapeutic agent with broad spectrum antitumor activity. It acts by inhibiting topoisomerase-II and activating oxidation/reduction reactions to produce derivatives that bind directly to DNA and cause DNA damage. Subsequently, prevent entry into the mitotic phase of cell division and promote apoptosis of the cancer cell [7]. Etoposide belongs to BCS Class IV category, has low solubility, erratic bioavailability with marked inter- and intra- subject variability and short biological half-life. It suffers from low selectivity and multidrug resistance with the potential risk of side effects. Therefore, the efficient drug delivery system is desired to overcome these drawbacks and improve its therapeutic effects [8].

The objective of present study was to develop an optimized formulation of etoposide-loaded gold nanoparticles (E-GN), with high stability and loading efficiency (LE), in order to improve etoposide therapeutic efficiency, selectivity and to control its release.

MATERIALS AND METHODS
Etoposide powder (98-105%) and gold nanoparticles suspensions with diameters of 5nm (GN5), 10nm (GN10) and 15nm (GN15) were purchased from Sigma-Aldrich Co., USA. Hydroxy propyl methyl cellulose E5 (HPMC-E5) was supplied from Provizer Pharma Co., India. Polyvinyl alcohol (PVA) was supplied from Panreac, Espana. All other ingredients used in the study were analytical grade. The labware was cleaned after each preparation using a freshly prepared aqua regia (1 part HNO_3 and 3 parts HCl) and deionized water (DW).

Preparation of Etoposide-Loaded gold nanoparticles (E-GN)
The preparation of E-GN suspensions comprised two main steps; the first was functionalized GN to enhance their dispersing capacity and improve etoposide LE, and then incorporated etoposide in to the functionalized GN [9].

Functionalization of GN

GN5 were functionalized by bio-conjugation method using HPMC-E5 and PVA with different concentrations, as shown in Table 1. Firstly, polymer solution was prepared by mixing an accurate amount of polymer with DW for 3h at 1500rpm. Then, the polymeric-gold nanoparticles (PGN) suspensions were prepared by mixing 0.5ml of polymer solution with 4.5ml of GN suspension, for 1h at room temperature (25°C) and 1500rpm; and sonicated for 6h. Then filtered using 0.1µm syringe-filter to remove the unconjugated polymers and any possible aggregates, and stored at 2-8°C in a tightly closed dark container for further studies [10].

AFM Measurement was used to infer the binding of polymer layer on the surface of GN and conclude about the stability of bio-conjugates as well as to evaluate the effect of polymer types and their concentrations on the GN growth and morphology.

Table 1. Composition of PGN suspensions.

Sample code	Polymer	
	Type	Concentration (mg/ml)
PGN1	HPMC-E5	5
PGN2		10
PGN3		15
PGN4		20
PGN5	PVA	5
PGN6		10
PGN7		15
PGN8		20
PGN9	HPMC-E5:PVA	5:5

Incorporation of Etoposide

Firstly a stock solution of etoposide was prepared by dissolving 0.15gm of etoposide in 0.5ml of dimethyl sulfoxide ((DMSO) and completed to 10ml by acetate buffer solution (pH 4.6), then sonicated for 3h at room temperature till a clear solution was obtained. 1ml of etoposide solution (at a calculated concentration) was added to 9ml of PGN suspension, and mixed for 1h at 1500rpm, then sonicated until a clear transparent suspension was achieved, and stored at 2-8°C in a tightly closed dark container, prior to further characterization [10,11]. Twelve formulas of E-GN were prepared, as shown in Table 2, adopting the above method, and optimized by studied the effect of the following variables:

1. Polymer type of PGN suspension
2. Temperature of incorporation Technique
3. Sonicating duration
4. Initial GN size
5. Etoposide loading

AFM measurement was used to evaluate the effect of the above variables on E-GN size, distribution and morphology. The zeta potential and TEM image of the optimized formula were evaluated to confirm the stability of E-GN as well as to interpret the exact shape and size of it.

Table 2. Composition of E-GN formulas.

Formula code	Polymer type	Temperature of incorporation technique	Sonication duration (hour)	pH of etoposide stock solution	Final Etoposide concentration (mg/ml)
F1	HPMC-E5	Room temperature	1	7.4	0.5
F2	PVA	Room temperature	1	7.4	0.5
F3	HPMC-E5:PVA	Room temperature	1	7.4	0.5
F4	HPMC-E5:PVA	45°C	1	4.6	0.5
F5	HPMC-E5:PVA	55°C	1	4.6	0.5
F6	HPMC-E5:PVA	65°C	1	4.6	0.5
F7	HPMC-E5:PVA	Room temperature	3	4.6	0.5
F8	HPMC-E5:PVA	Room temperature	5	4.6	0.5
F9 [1]	HPMC-E5:PVA	Room temperature	5	4.6	0.5
F10 [2]	HPMC-E5:PVA	Room temperature	5	4.6	0.5
F11 [1]	HPMC-E5:PVA	Room temperature	5	4.6	1
F12 [1]	HPMC-E5:PVA	Room temperature	5	4.6	1.5

[1] Formula prepared from GN10; [2] Formula prepared from GN15; other formulas were prepared from GN5

Evaluation of Etoposide LE

0.5ml of E-GN suspension was centrifuged with Amicon filter of 3KDa/MWCO, at 6000rpm for 20min. The amount of free etoposide was determined by UV-Visible measurement, and then calculated the etoposide LE by the following equation:

$$LE_{\%} = \frac{D_0 - D_f}{D_0} \times 100\% \quad (1)$$

Where $LE_{\%}$ is the percentage of drug loading efficiency, D_0 is the total amount of drug fed in formula and D_f is the amount of free drug leak through Amicon filter [12].

Evaluation of In-Vitro Etoposide Release

2ml of E-GN suspension was added into dialysis tubing of 12KDa/MWCO, and then immerged in a release jar filled with 500ml of release media at 37±1°C, and rotated at 100rpm. Samples of 3ml were withdrawn at predetermined time intervals of 0.25, 0.5, 0.75, 1, 1.5, 2, 3, 4, 5, 10, 15, 20 and 24hours. The samples were analyzed for etoposide content using UV-Visible spectrophotometer. The percentage of drug released was calculated by the following equation:

$$D_{\%} = \frac{D_t}{D_0} \times 100\% \quad (2)$$

Where $D_{\%}$ is the percentage of drug release at time t, D_t is the amount of drug release at certain time interval and D_0 is the total amount of drug fed in formula.

The pH-responsive capacity of E-GN was investigated using two different release media (phosphate buffer pH 7.4 and acetate buffer pH 4.6) [13].

In-vitro Cytotoxicity Study

MTT assay was performed to study the cytotoxicity of the optimized E-GN by comparing with the cytotoxicity of free etoposide as well as the blank GN10. NCI-H69 and BEAS-B2 cell lines were seeded at $1x10^4$ cells/well, using 96-well plates, and incubated at 37°C in 5%CO_2 humidified atmosphere for 24h until a confluent monolayer was acheived. The cells were treated with 200µl of pure etoposide and the optimized E-GN, with increasing etoposide concentrations (10, 15 and 20µg/ml) in addition to the blank GN10. The plates were incubated for 24, 48 and 72hours. 20µl of (5mg/ml) MTT was added to each well and incubated for 4hours at 37°C. The medium was carefully removed from wells to avoid dislodging the formazan crystals formed in the bottom. 200µl of DMSO was added to dissolve the crystals. The color intensity value of the processed cells was measured at the maximum absorbance of 550nm, using a spectrophotometric microplate reader, that present the cell survival and the inhibition rate percentages in corresponding wells in contrast with their respective controls, and calculated according to the following equations:

$$V_{\%} = \frac{A_t}{A_c} \times 100\% \quad (3)$$

$$I_{\%} = \frac{A_c - A_t}{A_c} \times 100\% \quad (4)$$

Where $V_{\%}$ is the percentage of cell viability of cell percentage, $I_{\%}$ is the percentage of cellular metabolic inhibition rate, A_t is the absorbance of the tested sample and A_c is the absorbance of the control [14,15].

RESULTS

Functionalization of GN

PGN suspensions were prepared using HPMC-E5 and PVA with concentration lower than 0.5mg/ml, gave a dark red color directly after preparation which subsequently, converted to a blue within about 1day, revealed to an aggregation of free GN [10]. Figure 1demonstrated the AFM analysis of the functionalized gold nanoparticles PGN1-9. Increased the particles size (PS) of PGN compared to GN5, with uniform particles size distribution (PSD), indicated that GN were indeed conjugated with polymer [16].

PGN1-8 showed a complex relationship between the polymer concentration and PS reduction. The PS and PSD was decreased significantly ($p<0.05$) by increased the polymer concentration from 0.5 to 1mg/ml, then; the PS and PSD started to increase significantly ($p<0.05$) above these concentration limits. The nonlinear concentration dependence happened due to the free GN was decreased with increased polymer concentration, leaded to decrease the possible aggregates of small GN through coordination bonds. While increased the polymer concentrations above the optimum limit leaded to formation large aggregates of individual PGN by intermolecular electrostatic interactions. PGN4 and PGN8 with higher polymer concentration of 20mg/ml for HPMC-E5 and PVA respectively, showed large PS with wide PSD, indicated for the formation of polymeric nanoparticles aggregates [10,11].

PGN9 was prepared from combination of HPMC-E5 and PVA at ratio 1:1, gave a smallest PS (average 13.78nm) with more uniform PSD of (18.56%), when compared with PGN of each polymer separately (PGN2 and PGN6), clarify that this combination improved the tendency of polymer coating to stabilized the GN by enhancement of the electrostatic repulsion forces.

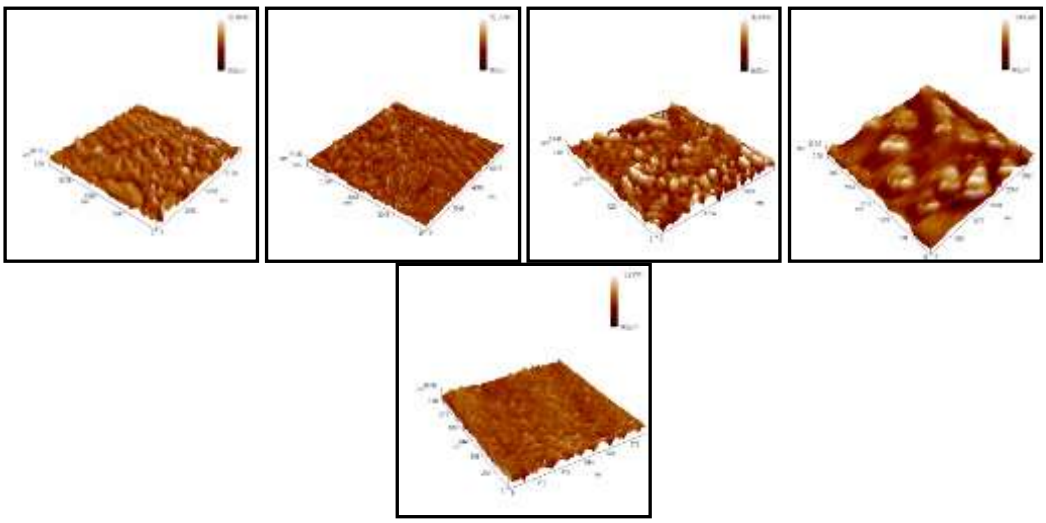

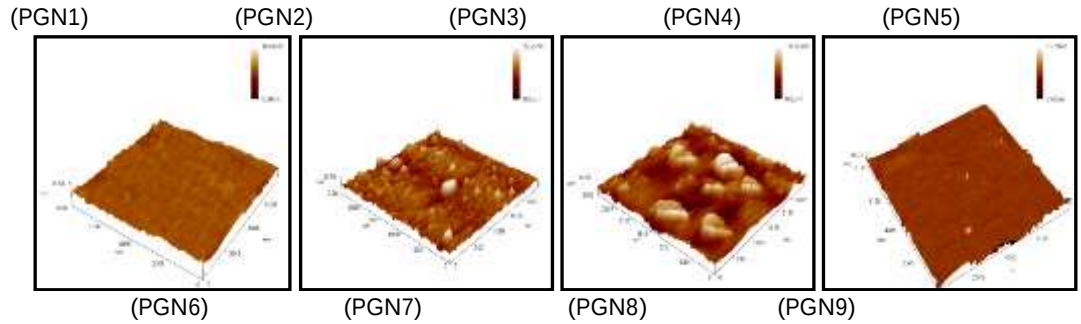

Figure 1. AFM 3D images PGN1-9

Incorporation of Etoposide

Twelve formulas of E-GN were prepared by incorporation technique. PGN2, PGN6 and PGN9 with ultra nano-size could give a high surface area for etoposide incorporation. These nanoparticles had a high loading capacity besides the presence of surface active groups that might form bonds with etoposide per unit area [17].

Optimization of E-GN

Effect of Polymer Type of PGN Suspension

The functionalized suspensions (PGN2, PGN6 and PGN9) were selected to prepare formulas F1-3 respectively, in order to study the effect of polymer types on E-GN. PS had an impact on the etoposide LE. The observations suggested that LE of nanoparticles increased with the decrease in PS. As a well-known fact; "lower the particle size more will be the availability of surface containing active sites for adsorption of drug" [18]. Consequently the LE of etoposide (Figure 2) for PGN was improved by using different polymers types and it was found in the following order:

HPMC-E5: PVA > PVA > HPMC-E5 as found in (F3, F2 and F1) respectively.

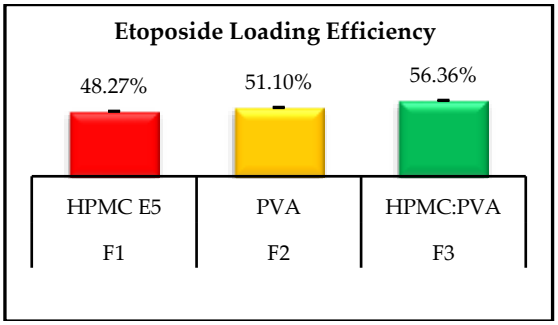

Figure 2. Etoposide LE of formulas F1-3 with different type of polymers (values are represented as mean% ± SD)

The AFM analysis (Figures 3) of formulas F1-3 revealed a significant increased ($p<0.05$) of PS and non-significant ($p>0.05$) increased of PSD when compared with the blank PGN2, PGN6 and PGN9 respectively, which indicated for the uniformity of drug loading and the efficacy of the incorporation technique.

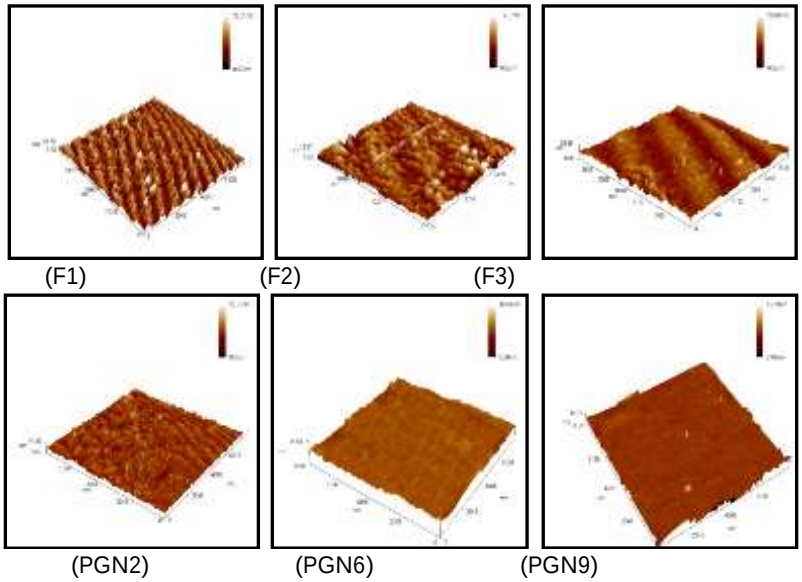

Figure 3. AFM 3D images for comparative the PS of formulas F1-3 with their polymeric suspensions PGN2, PGN6 and PGN9 respectively

The release profile of formula F1 containing HPMC-E5, as shown in Figure 4, showed a very low etoposide release rate in both phosphate buffer (pH 7.4) and acetate buffer (pH 4.6), related to the stability of polymer under changing the pH of release media, making a high retardation for drug release. On the other hand the release profile of formula F2 containing a pH sensitive polymer (PVA) showed a weak etoposide retarding at pH 7.4 and overmuch release rate at pH 4.6 with burst releasing the active ingredient within less than 15 minutes. The release profiles of formulas F3 containing a combination of HPMC-E5 and PVA polymers, showed a better etoposide retardation at pH 7.4 and greater release rate with controlled manner at pH 4.6 [19,20]. The results indicated that LE and in-vitro release profile of etoposide were improved significantly ($p<0.05$) when used a combination of HPMC-E5 and PVA polymers (F3), as compared with other formulas containing a single non-ionic polymer of HPMC-E5 (F1) or PVA (F2) separately. Formulas F3 was selected for further optimization studies.

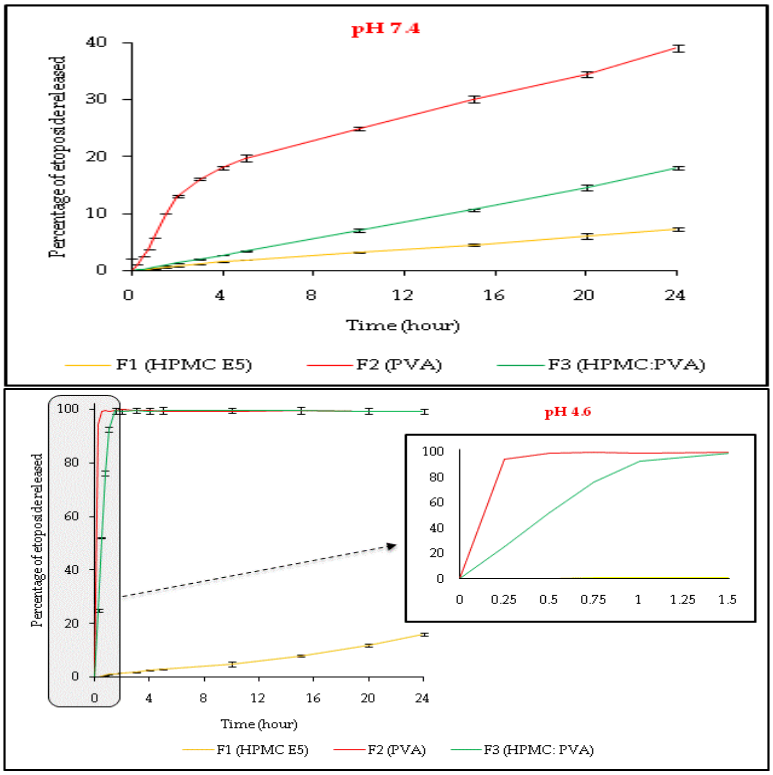

Figure 4. Release profile of etoposide from formulas F1-3 in phosphate (pH 7.4) and acetate (pH 4.6) buffer solutions at 37 ± 1 °C (data are represented as mean% ± SD for n=3)

Effect of Temperature of Incorporation Technique

In order to determine an appropriate temperature of incorporation technique, different temperatures (room temperature, 45°C, 55°C, and 65°C) were employed in the preparation of formulas F3-6, respectively. Etoposide LE was significantly decreased ($p<0.05$) with increased the temperature of incorporation technique, as shown in Figure 5. The reason behind this result related to the conformation of polymers chains in aqueous solution; which became more stretched at elevated temperature leading to decrease the adsorption of etoposide on the polymeric surface of GN [19,21].

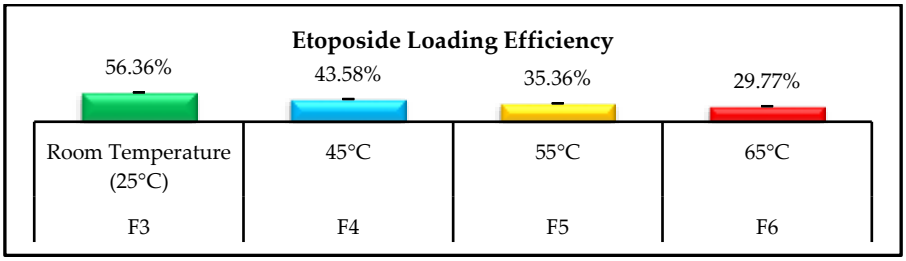

Figure 5. Etoposide LE of formulas F3-6 with different incorporated temperature (values are represented as mean% ± SD)

AFM analysis (Figure6) revealed a significant increased ($p<0.05$) in PS and PSD with increased the temperature of incorporation technique, in spite of the decreased of etoposide LE, which indicated for the tendency of nanoparticles to aggregate via elevation of temperature. Formula F3 gave a better etoposide LE, PS and PSD, was chose for further optimization studies.

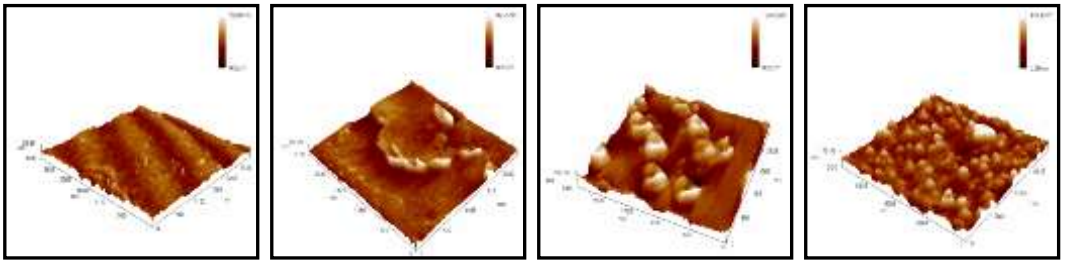

(F3) (F4) (F5) (F6)

Figure 6. AFM 3D images of formulas F3-6

Effect of Sonicating Duration

The effect of sonicating duration of incorporation technique was evaluated using different durations (1, 3 and 5 hours) for formulas F3, F7 and F8, respectively. E-GN prepared without sonication gave nanoparicles with very bad LE (less than 7%), Indicated that etoposide loading was substantially affected by sonicating the suspension during the surface loading process [22]. Etoposide LE (Figure 7) and thereby PS and PSD (Figure 8) were improved significantly ($p<0.05$) by increasing the sonicating duration. Non significantly improvement ($p>0.05$) in etoposide release profile (Figure 9) was found by increased the sonicating duration of incorporation technique. Formula F8 was selected for further optimization studies.

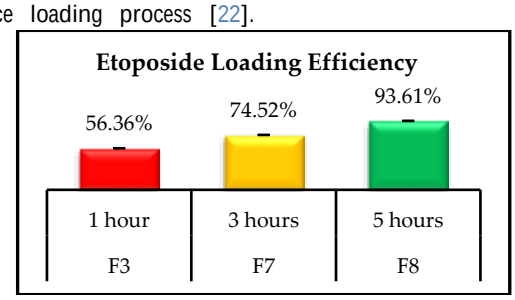

Figure 7. Etoposide LE of F3, F7 and F8 with different sonicating duration (values are represented as mean% ± SD)

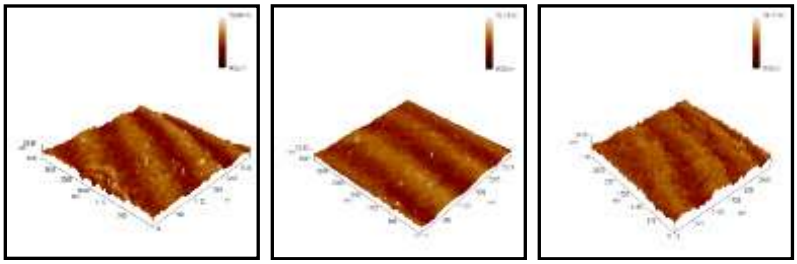

(F7) (F7) (F8)

Figure 8. AFM 3D images of formulas F3, F7 and F8

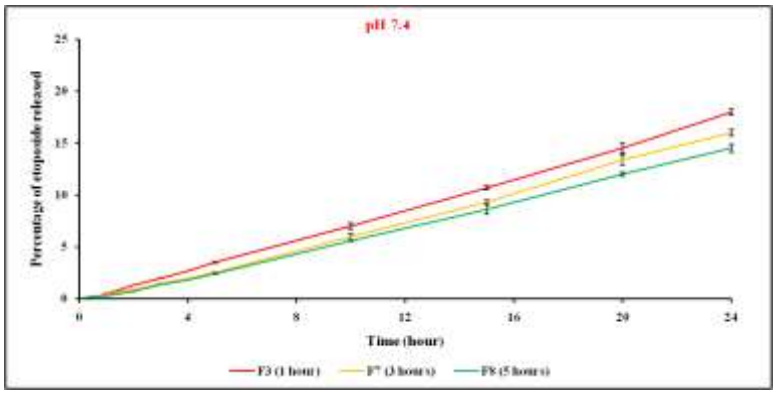

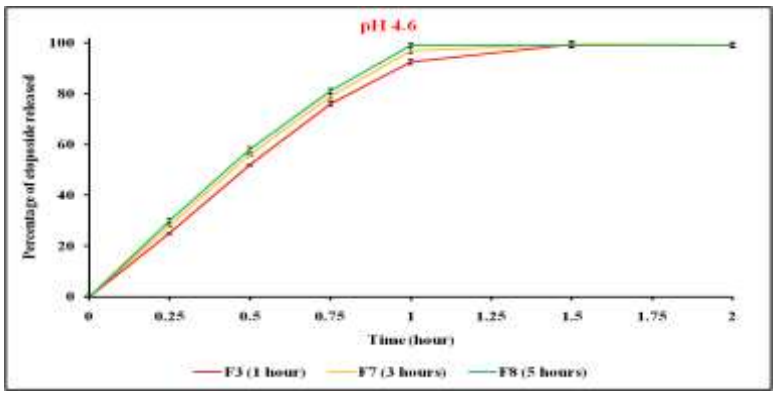

Figure 9. Release profile of etoposide from formulas F3, F7 and F8 in phosphate (pH 7.4) and acetate (pH 4.6) buffer solutions at 37 ± 1 °C (data are represented as mean% ± SD for n=3)

Effect of Initial GN Size

The effect of initial GN size on E-GN was investigated using three types of GN (GN5, GN10 and GN15), which functionalized previously with (HPMC-E5: PVA combination). Etoposide LE (Figure 10) of formula prepared from GN10 (F9) was higher than that of formulas prepared from GN5 (F8) and GN15 (F10). This result might due to the susceptibility of GN5 with smaller size of about 5nm to form larger nanoparticles through the coating process [23]; which illustrated by the higher PSD (Figure 11) of formulas prepared from GN5 comparing to these prepared from GN10 or GN15. AFM analysis (Figures 11) showed a significant improvement ($p<0.05$) in PSD of formula F10. The release profile (Figure 12) was not significantly affected ($p>0.05$) by changing the initial GN sizes. Formula F10 was selected for further optimization studies.

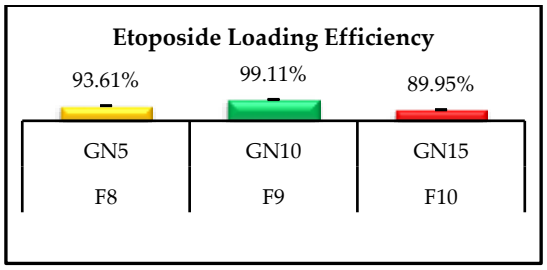

Figure 10. Etoposide LE of E-GN formulas F8-10 with different initial GN size (values are represented as mean% ± SD)

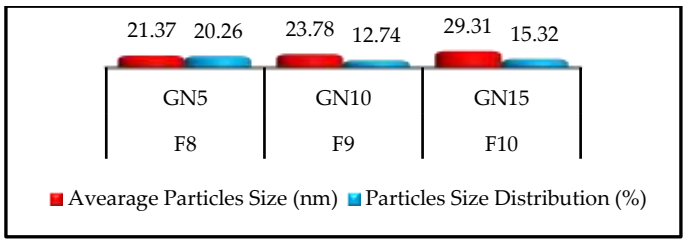

Figure 11. AFM average PS and percentage of PSD F8-10

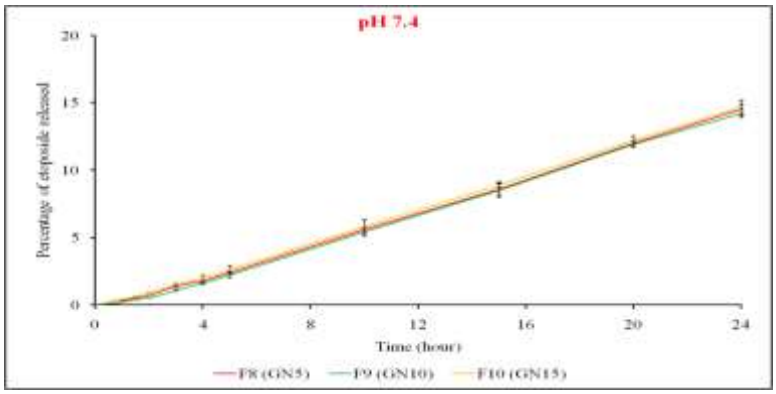

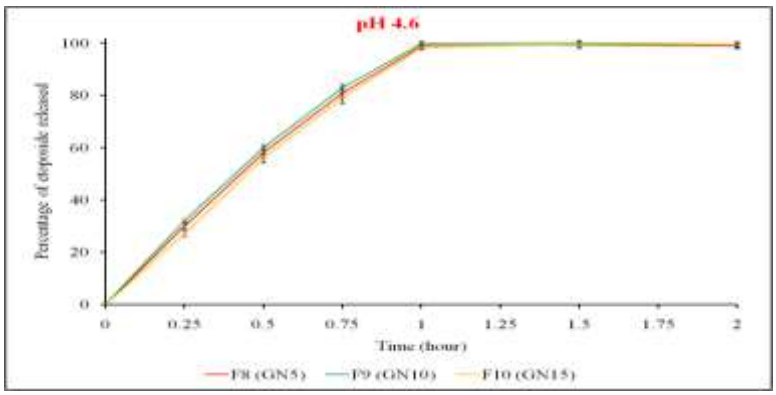

Figure 12. Release profile of etoposide from formulas F8-10 in phosphate (pH 7.4) and acetate (pH 4.6) buffer solutions at 37 ± 1 °C (data are represented as mean% ± SD for n=3)

Effect of Etoposide Loading

Formulas (F9, F11 and F12) were prepared with different etoposide concentrations of 0.5, 1 and 1.5mg/ml, respectively. Formula F11 showed maximum loading capacity (1mg/ml etoposide) with higher LE (99.57%), analysis (Figures 24-26) revealed a significant improved ($p<0.05$) in PS of formula F11 with 1mg/ml etoposide, comparing to F9 with 0.5mg/ml etoposide (figures not shown).

According to the results of all studies, formula F11 with best etoposide LE, in-vitro release profile, PS and PSD, considered as the optimized E-GN.

TEM image (Figure 13) of the optimized formula (F11) revealed uniform spherical nanoparticles with average size of 27.92nm [24]; the data was not significantly ($p>0.05$) differed than the data of AFM analysis. Formula F11 revealed a highly negative zeta potential of -39.23 [25]. F11 would be struggle against aggregation due to a strange repellent force between particles.

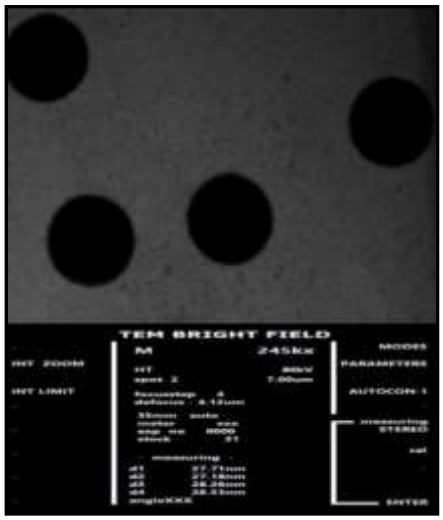

Figure 13. TEM 2D image of the optimized formula F11

In-vitro Cytotoxicity Study

United State FDA was approved etoposide as a first line treatment for patient with limited stage small cell lung cancer (SCLC). A standard etoposide IV dose of 100-140mg/m^2 would result in a peak plasma concentration of 10-20µg/ml. Therefore, etoposide was used at 10, 15 and 20µg/ml to represent clinically relevant dosing. The cytotoxicity effect of all samples against the cell lines used was depended mainly on the pathway of penetration through the cells. Free etoposide penetrated the cells membrane passively, while the GN internalized by cells via endocytosis process, and subsequently degraded by the acidic pH (about 4.6) of lysosomes and the metalloproteinase enzymes. Overexpresion of receptors mediated endosytosis and cytoplasmic enzymes considered as the hallmarks of cancer [26,27].

Figure (14-A) demonstrated the cytotoxicity assay against NCI-H69 cell line with SCLC. The blank GN10 showed a limited anticancer activity with $V_{\%}$ more than 70%, related to the relatively toxic metal ions triggered through biodegradation of GN, which affected the cell homeostasis and functions [28]. F11 showed a significant ($p<0.05$) improved of cytotoxicity effect (lower $V_{\%}$) as compared with free etoposide, at all concentrations used (10, 15 and 20µg/ml) and at different times of exposure (24, 48 and 72hours). This due to E-GN enhanced the penetration of etoposide to cancer cells and released it in slow and continuous (controlled) manner, in addition to the synergistic activity of GN10.

GN have much smaller PS that preferentially accumulated at the cancer site mediated by passive targeting; exploits abnormal gap junctions in the epithelium of cancer blood vessels and altered lymphatic drainage [29]. BEAS-B2 cell line of normal bronchial epithelium used to evaluate the undesirable cytotoxic effect of samples against healthy cells that neighboring the cancer. The same samples concentrations and times of exposure were applied. In all cases, the loading of etoposide on GN led to significantly

($p<0.05$) reduced the undesirable cytotoxic effect (low $I_{\%}$) of etoposide on normal cell line (Figure 14-B). This could be attributed to decreased permeability and increased resistance of normal cells toward etoposide in its complex form with GN.

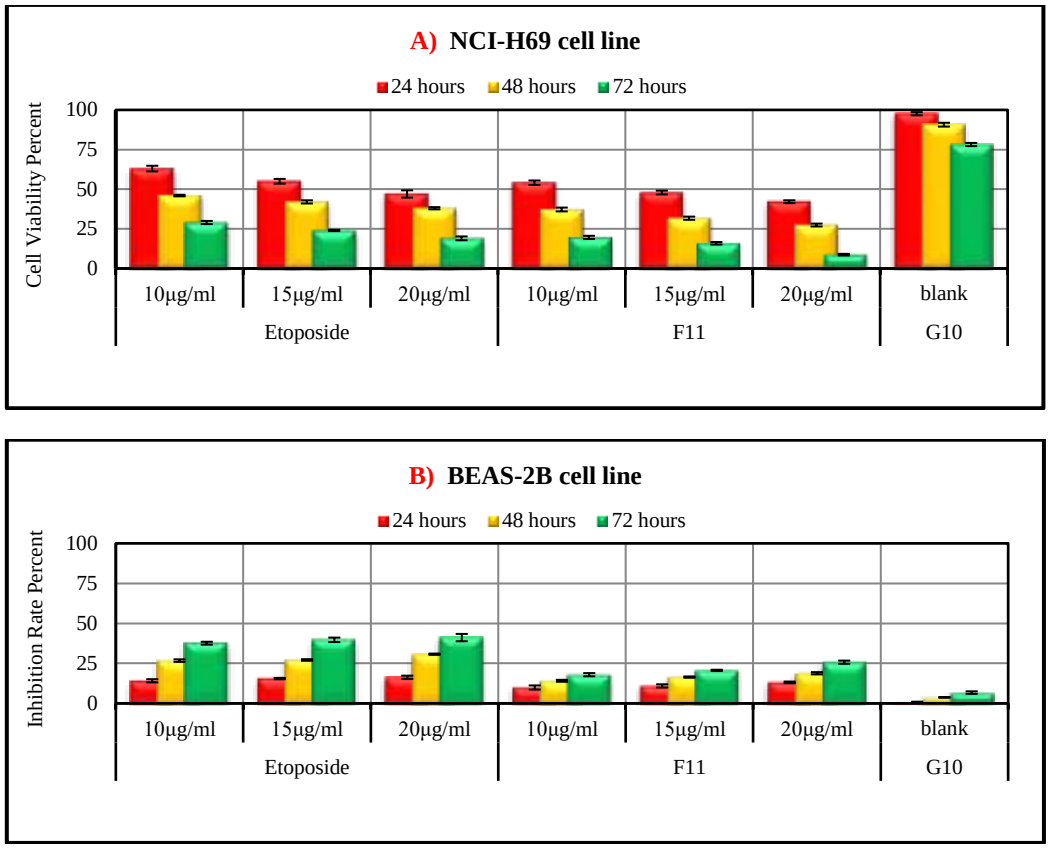

Figure 14. In-vitro cytotoxicity comparasion of pure etoposide, blank GN10 and the optimized E-GN (F11) on: (A) NCI-H69; (B) BEAS-B2 cell lines, in response to three etoposide concentrations of 10, 15 and 28µg/ml and after 24, 48 and 72 hours of exposure. Data points represented as mean% ± SD

CONCLUSIONS

Functionalization of GN was improved the colloidal stability and allowed incorporation of etoposide with high loading capacity. E-GN prepared from GN10, which functionalized with a combination of HPMC-E5 and PVA at ratio (1:1), gave higher etoposide LE, best particles uniformity and controlled in-vitro release. In-vitro cytotoxicity assay showed much more selectivity of E-GN toward cancer (NHI-H69) than normal (BEAS-B2) cell lines. Indicated that GN system harnesses the peculiar endocytic system of cancer could be used in favor of effective patient treatment.

All these results gave a preliminary indication that E-GN was reliable candidate to be effective multiplexed therapeutic agent. Therefore, we encourage to extension of future research to include studying the pharmacokinetic profile and performing in-vivo toxicity studies.

REFERENCES

1. Valerio V. *Update on Gold Nanoparticles: From Cathedral Windows to Nanomedicine*, Smithers Rapra Technology, 2013.
2. Mei, W. et al. Applications of metal nanoparticles in medicine/metal nanoparticles as anticancer agents. In *Metal Nanoparticles: SAPS*, 2018; pp. 169–190.
3. Balakrishnan, S. et al. A. Applications of Gold Nanoparticles in Cancer. In *Biomedical Engineering: CMTA*, 2018; pp. 780-808.
4. Fu, L.H.et al. Synthesis of gold nanoparticles and their applications in drug delivery. In *Metal Nanoparticles in Pharma*, 2017; pp. 155-191.
5. Lombardo, D. et al. Smart nanoparticles for drug delivery application: development of versatile nanocarrier platforms in biotechnology and nanomedicine. *JNM* 2019, *2019*.
6. Long, B.H. Structure-activity relationships of podophyllin congeners that inhibit topoisomerase II. *NCI Monographs* 1987, *4*, 123-127.
7. Choudhury, H. et al. Advanced nanoscale carrier-based approaches to overcome biopharmaceutical associated with anticancer drug 'Etoposide'. *MSEC* 2019, *106*, 110275.
8. Suarasan, S. et al. Gelatin-coated Gold Nanoparticles as Carriers of FLT 3 Inhibitors for Acute Myeloid Leukemia Treatment. *CBDD* 2016, *87*, 927-935.
9. Banu, H.et al. Doxorubicin loaded polymeric gold nanoparticles targeted to human folate receptor upon laser photothermal therapy potentiates chemotherapy in breast cancer cell lines. *JPPB* 2015, *149*, 116-128.
10. Suarasan, S. et al. Doxorubicin-incorporated nanotherapeutic delivery system based on gelatin-coated gold nanoparticles: formulation, drug release, and multimodal imaging of cellular internalization. *ACS AMI* 2016, *8*, 22900-22913.

11. Khodashenas, B. et al. Gelatin–Gold Nanoparticles as an Ideal Candidate for Curcumin Drug Delivery: Experimental and DFT Studies. *JIOPM* 2019, *29*, 2186-2196.
12. Haddada, M. B.et al. Novel Synthesis and Characterization of Doxycycline-Loaded Gold Nanoparticles. *PPSC* 2019, *36*, 1800395, 1-11.
13. Amanlou, N. et al. Enhanced cytotoxic activity of curcumin on cancer cell lines by incorporating into gold/chitosan nanogels. *MCP* 2019, *226*, 151-157.
14. Lin, Y. et al. Effect of sun ginseng potentiation on epirubicin and paclitaxel-induced apoptosis in human cervical cancer cells. *JGR* 2015, *39*, 22-28.
15. Jabir, M.S. et al. Novel of Nano Delivery System for Linalool Loaded on Gold Nanoparticles Conjugated with CALNN Peptide for Application in Drug Uptake and Induction of Cell Death on Breast Cancer Cell Line. *MSEC* 2019, *94*, 949–964.
16. Lay-Ekuakille, A. et al. Conductivity Image Characterization of Gold Nanoparticles based-Device through Atomic Force Microscopy. *NANOfIM,* 2018, 1-6.
17. Kong, F.Y. et al Unique roles of gold nanoparticles in drug delivery, targeting and imaging applications. *Molecules* 2017, *22*, 1445, 1-13.
18. Devrim, B. et al. Preparation and evaluation of modified release ibuprofen microspheres with acrylic polymers by quasi emulsion solvent diffusion. *APPDR* 2006, *63*, 521-534.
19. Sahoo, C.K. et al. HPMC a biomedical polymer in pharmaceutical dosage forms. *JPS* 2015, *8*, 875-81.
20. Madhusudhan, A. et al. Efficient pH dependent drug delivery to target cancer cells by gold nanoparticles capped with carboxymethyl chitosan. *IJMS* 2014, *15*, 8216-8234.
21. Wiśniewska, M. Temperature effects on the adsorption of polyvinyl alcohol on silica. *Open Chem* 2012, *10*, 1236-1244.
22. Nawaz, M. et al. Preparation, morphology and sonication time dependence of silver nanoparticles in copolymers of PEO with polystyrene or PMMA. *JPR* 2017, *24*, 137, 1-8.
23. Chen, Y. et al. Highly sensitive determination of dopamine based on the aggregation of small-sized gold nanoparticles. *Microchem J* 2019, *147*, 955-961.
24. Mohamed, A.I. et al. Preparation and characterization of cytotoxic drug loaded gold nanoparticles. *Ijppr* 2016, *6*, 640-652.
25. Reznickova, A. et al. PEGylated gold nanoparticles: Stability, cytotoxicity and antibacterial activity. *Colloids Surf A Physicochem Eng Asp* 2019, *560*, 26-34.
26. Lawson, M.H. et al. Two novel determinants of etoposide resistance in small cell lung cancer. *Cancer res* 2011, *71*, 4877-4887.
27. Teicher, B. A. et al. Small cell lung carcinoma cell line screen of etoposide/carboplatin plus a third agent. *Cancer med* 2017, *6*, 1952-1964.
28. Yah, C.S. The toxicity of Gold Nanoparticles in relation to their physiochemical properties. *Biomed Res* 2013, *24*, 400-413.
29. Morales-Cruz, M. et al. Smart Targeting To Improve Cancer Therapeutics. *DDDT* 2019, *13*, 3753, 1-19.